Title
Carrier Transport in Artificially Structured Two-Dimensional Semiconductor

Author
Walukiewicz, W.

Publication Date
1992

LBL-32141
UC-404

Center for Advanced Materials

CAM

To be published as a chapter in *Semiconductor Interfaces and Microstructure*, Z.C. Feng, editor, World Scientific Publishing Co. PTE Ltd., Republic of Singapore, 1992

Charge Carrier Transport in Artificially Structured Two-Dimensional Semiconductor Systems

W. Walukiewicz

March 1992

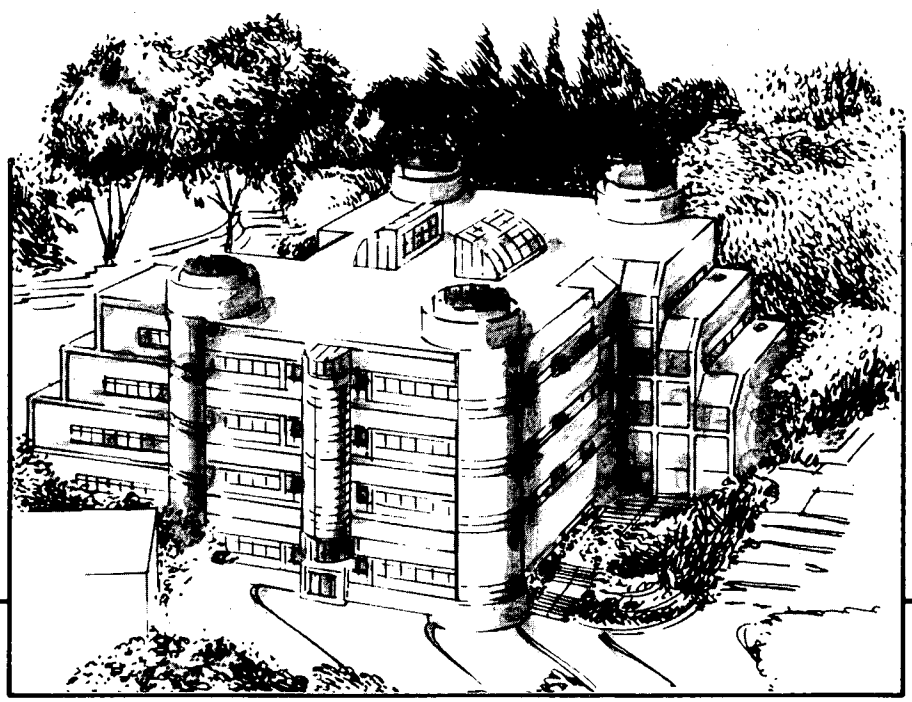

Materials and Chemical Sciences Division

Lawrence Berkeley Laboratory • University of California

ONE CYCLOTRON ROAD, BERKELEY, CA 94720 • (415) 486-4755

Prepared for the U.S. Department of Energy under Contract DE-AC03-76SF00098

DISCLAIMER

LBL-32141
UC-404

Charge Carrier Transport in Artificially Structured Two-Dimensional Semiconductor Systems

W. Walukiewicz

Center for Advanced Materials
Materials Sciences Division
Lawrence Berkeley Laboratory
University of California
Berkeley, CA 94720

March 1992

This work was supported by the Director, Office of Energy Research, Office of Basic Energy Sciences, Materials Sciences Division, of the U.S. Department of Energy under Contract No. DE-AC03-76SF00098.

CHARGE CARRIER TRANSPORT IN ARTIFICIALLY STRUCTURED TWO-DIMENSIONAL SEMICONDUCTOR SYSTEMS

W. Walukiewicz
Center for Advanced Materials, Materials Sciences Division
Lawrence Berkeley Laboratory, University of California
1 Cyclotron Road, Berkeley, California 94720 USA

ABSTRACT

Transport of electrons and holes in two-dimensional and quasi-three-dimensional semiconductor systems is reviewed. Contributions of different scattering processes to the total electron and hole mobilities in various types of modulation doped heterostructures are calculated. It is shown that in a wide temperature range phonon scattering is the principal scattering mechanism limiting electron and hole mobilities in high quality AlGaAs/GaAs modulation doped heterostructures. The importance of nonspecular scattering from rough walls in wide parabolic wells is emphasized. Also, several unresolved or poorly understood aspects of charge transport in two-dimensional semiconductor systems are discussed.

1. INTRODUCTION

The last decade has witnessed an unprecedented growth of research on low dimensional semiconductor systems. Sophisticated epitaxial techniques such as Molecular Beam Epitaxy, Metalorganic Chemical Vapor Deposition and numerous variations of these two growth methods allow atomic scale control of the growth process and are widely used to grow these complex semiconductor structures. Since all the epitaxial techniques provide excellent control of composition and doping only along the growth direction, they are used most successfully to fabricate two dimensional structures. Additional confinement in the growth plane is much more difficult to achieve and control. Therefore, although substantial progress has been made in the last few years, studies of truly one- and zero-dimensional semiconductor systems are still quite rare.

Low dimensional semiconductor systems have become fertile ground for basic research. The discovery of the Quantum Hall Effect [1] and the Fractional Quantum Hall Effect [2] were major developments in fundamental solid state physics in the last several years. Flexibility with which various structures could be designed and practically realized has led to new concepts of charge transport in mesoscopic systems. Also, a wealth of new linear and nonlinear optical effects has been observed in semiconductor quantum wells [3].

One of the most basic characteristics of a semiconductor system is its response to the external fields. This response is determined by the properties of

in mesoscopic systems. Also, a wealth of new linear and nonlinear optical effects has been observed in semiconductor quantum wells [3].

One of the most basic characteristics of a semiconductor system is its response to the external fields. This response is determined by the properties of the semiconductor material as well as by specifics of the interaction of the charge carriers with collective excitations and imperfections of the crystal lattice. Studies of the electronic transport in three-dimensional (3D) semiconductors have provided invaluable information on a variety of semiconductor band structure parameters [4]. In addition, in many instances an analysis of the free carrier mobility has been used to determine the strength of the charge carrier scattering potentials [5,6].

It was evident from the beginning that the introduction of artificially structured 2D systems would open an opportunity to study basic transport phenomena in a new and in many respects unusual material systems [7]. Using the concept of modulation or selective doping it has been possible, for the first time, to separate charge carriers from the parent impurities [7,8]. This concept led to a very substantial reduction of impurity scattering and allowed the study of charge transport in almost perfectly pure semiconductors where phonon scattering plays a dominant role down to very low temperatures.

There are several review papers on properties of 2D systems. Ando *et al.* [9] have reviewed the progress in the field of 2D systems until the early 1980's. Understandably, at that time most of the work was limited to studies of 2D inversion layers in Si and InAs. However, the main theoretical concepts presented in the review can be easily adopted to any 2D system. Recently, various aspects of modulation doped semiconductor systems were reviewed in a series of articles covering basic properties of modulation doped structures [10] as well as their applications for electronic [11] and optoelectronic devices [12,13].

The main objective of this review is to present recent theoretical and experimental results on electronic transport in 2D and quasi-3D modulation doped heterostructures. We will focus our attention on 2D electron or hole gases confined at heterointerfaces of different semiconductors. However, many of the concepts and results will be directly applicable to charge transport in any two dimensional system. The basic theoretical concepts will be illustrated with experimental results on the most extensively studied material systems. Due to the limited scope of the review, we will refrain from discussing lattice mismatched systems where strain plays a significant role in determining electronic structure and transport properties [14].

The material in this chapter is structured as follows: The background information on the electronic structure of electron and hole gases confined in thin 2D films is presented in section 2. In section 3 and 4 the scattering processes limiting carrier mobilities are introduced and the differences in carrier scattering in 2D and quasi-3D systems are discussed. Calculated electron and hole mobilities in various modulation doped materials systems are compared with representative experimental data in section 5. Finally the discussion of currently

actively studied, and possible future research areas are discussed in the closing section 6.

2. ELECTRONIC STRUCTURE

Quantum confinement of electrons and holes in 2D planes can be achieved by several methods. Charge carriers can be confined in an accumulation or inversion layer at a semiconductor surface [15]. The carriers can also be confined by an attractive electrostatic potential created by δ or planar doping [16]. However, the method most widely used to produce 2D systems utilizes band offsets at semiconductor heterointerfaces [17]. The band offsets can be used to confine electrons or holes in a thin square quantum well or at a interface between two different semiconductors. Modern epitaxial techniques provide an atomic scale control over the thickness of the films and the smoothness of the interfaces. The value of the available band offset depends on the semiconductor materials and for III-V compounds may be as large as 1.3 eV [18].

In order to achieve 2D confinement the system has to satisfy certain conditions. First, the thickness of the well has to be smaller than the electron or hole de Broglie wavelength. For a 3D electron or hole gas of concentration n the de Broglie wavelength at the Fermi energy is $\lambda_F = 2\pi/k_F$, where $k_F=(3\pi^2 n)^{1/3}$. Hence the condition to observe 2D confinement of such gas is that the thickness w of the well satisfies the condition

$$w < 2\left(\frac{\pi}{3n}\right)^{1/3} \qquad (1)$$

It should be emphasized that this is a universal condition which does not depend on any semiconductor material parameters.

Another characteristic length for an electron or hole gas is the mean free path, i.e., the distance an electron or a hole can travel between momentum randomizing scattering events. For a 2D gas the mean free path l_p has to satisfy the condition,

$$l_p = v_F \cdot \tau = \hbar k_F \mu/e = \hbar (3\pi^2 n)^{1/3}\mu/e > w \qquad (2)$$

where v_F is the carrier velocity at the Fermi level, τ is the relaxation time and μ the mobility. The above condition has a simple physical interpretation: it states that in a 2D system electrons or holes interact with the confinement walls more frequently than with random scattering centers.

In general, for low effective mass high mobility carriers, condition (1) is more restrictive than condition (2). For example, to observe a 2D gas in GaAs with 10^{17} cm^{-3} charge carriers $\lambda_F \cong 440$ Å and a plane confinement of a width smaller than 400 Å is required. On the other hand, for a carrier concentration of 10^{17} cm^{-3} the low temperature electron mobility easily exceeds 10^4 cm^2/Vs. Therefore, in this case the condition (2) is satisfied for w<1000 Å. It can be

shown that in most semiconductor systems a confinement of the order of 100 Å is necessary to clearly observe quantum effects. Such a degree of confinement is easily accessible and can be practically realized in many semiconductor systems.

Recently a new type of structure which connects 2D with 3D limits has been proposed and practically realized. In so-called parabolic quantum wells a wide well can be obtained by a combination of proper design of the alloy composition in the well with remote doping [19,20]. The width of such wells can be of the order of 1000 Å, i.e., it is larger than the de Broglie wavelength. Therefore, although the carrier motion is not quantized the mean free path in such structure can be larger than the width of the well. Consequently, one has to account for an interaction of free carriers with the confinement walls.

Among the variety of possible 2D semiconductor systems the single quantum well modulation doped heterostructures (SQW-MDH) are the semiconductor structures most frequently used to study transport of 2D electrons and/or hole gases. In such structures, schematically shown in Fig. 1, the shallow donors or acceptors are located in the barrier forming semiconductor S2. The carriers are transferred from the parent dopants into the well forming semiconductor S1. The resulting electric field confines the mobile charges in a narrow quasi-triangular well at the heterointerface. By changing the distance d separating the dopants from the quantum well one can control the concentration of the electrons or holes in the well. Also, by increasing the separation one is able to very substantially enhance the carrier mobility by reducing the effectiveness of the ionized impurity scattering. Practical implementation of this idea has resulted in n-type AlGaAs/GaAs MDHs with low temperature electron mobilities exceeding 10^7 cm^2/V•s [21,22] and p-type structures with hole mobilities approaching 4×10^5 cm^2/V•s [23]. The principal objective of all theoretical calculations of the 2D transport is to understand the scattering mechanisms limiting electron and hole mobilities in such structures. The starting point

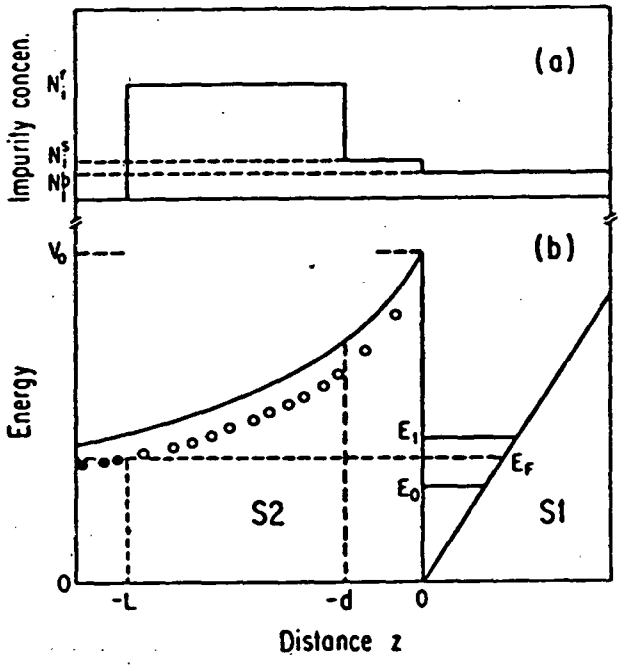

Fig. 1:Schematic representation of (a) the doping profile and (b) the energy configuration for a n-type, single quantum well modulation doped heterostructure. (After ref. [26])

of the theory is to provide an accurate description of the electronic structure of electrons or holes confined in a quasi-triangular quantum well at the heterointerface.

2.1 Electronic Structure of n-type MDH

The wavefunction of an electron gas confined in the z-direction can be written in the form,

$$\Psi_{n,\vec{k}}(\vec{r},z) = \frac{1}{L^2}\chi_n(z)\exp\left(i\vec{k}\cdot\vec{r}\right) \tag{3}$$

where $\vec{R} = (\vec{r},z)$, $\vec{r} = (x, y)$ and $\vec{k} = (k_x, k_y)$. The wavefunction $\chi_n(z)$ is given by the solution of coupled Schrödinger and Poisson equations [24,25],

$$-\frac{\hbar^2}{2m^*}\frac{d^2}{dz^2}\chi_n(z) + \left[V_0\theta(-z) - e\phi(z)\right]\chi_n(z) = E_n\chi_n(z) \tag{4}$$

$$\frac{d^2}{dz^2}\phi(z) = \frac{4\pi e^2}{\varepsilon_0}\left[\sum_{i=0}^{m} N_i\chi_i(z) + N_A(z) - N_D(z)\right] \tag{5}$$

Here $E_n(\vec{k}) = E_n + \hbar^2\vec{k}^2/2m^*$ is the dispersion relation for the n-th subband. $V_0\theta(-z)$ represents a step-like band offset at z=0. $N_D(z)$ and $N_A(z)$ are the functions representing the distribution of shallow donors and acceptors respectively, N_i is the density of electrons in the i-th subband. In the present approximation the exchange-correlation potential has been neglected. It has been shown that this potential does not play a significant role in AlGaAs/GaAs like MDHs [24]. The distribution of localized charges is schematically represented in Fig. 1 and is given by,

$$N_D(z) - N_A(z) = \begin{cases} N_i^b & z>0 \\ N_i^s & -d<z<0 \\ N_i^r & -L<z<0 \end{cases} \tag{6}$$

Here we assume a constant, z-independent concentration of dopants in each of the considered regions. In general, solutions of Eqs. (4) and (5) require numerical calculations. However, it has been shown that in the case of heterostructures shown in Fig. 1, an approximate variational solution can be obtained. The wave function of the ground subband can be represented by [25],

$$\chi_0(z) = \begin{cases} Bb^{1/2}(bz+\beta)\exp\left(-bz/2\right) & z>0 \\ B'b'^{1/2}\exp\left(+b'z/2\right) & z<0 \end{cases} \qquad (7)$$

where B, b, B′, b′ and β are variational parameters related to each other through the boundary conditions at the heterointerface, and the normalization condition for χ_0 (z). Therefore the parameters B, B′ and β can be expressed in terms of b and b′ [27]. The corresponding energy E_0 of the bottom of the ground subband depends in a complex way on the variational parameters and the details of the carrier and impurity distribution in the MDH [27].

The part of the wavefunction for $z < 0$ represents the finite penetration of the electron gas into the barrier. Incorporation of the penetration is important for calculations of the alloy disorder and surface roughness scatterings in GaAlAs/GaAs MDHs. The variational wavefunction (7) is very frequently used in the calculations of the electronic transport at low electron densities when only the ground subband is occupied [25,27]. At higher electron densities or at elevated temperatures one needs to consider also the transport in higher lying excited subbands [26]. An exact treatment of such a problem is rather difficult and requires extensive numerical calculations. An approximate description of the two band transport will be discussed later.

In numerous attempts to calculate the electron mobility in MDHs, an even simpler approach has been used in which the penetration of the wavefunction into the barrier is ignored. In such a case the ground state subband wavefunction takes the form [9,28],

$$\chi_0(z) = \begin{cases} \left(\frac{b_0^3}{2}\right)^{1/2} z\exp\left(-b_0 z/2\right) & z>0 \\ 0 & z<0 \end{cases} \qquad (8)$$

The parameter b_0 has a simple form [28],

$$b_0^3 = \frac{33\pi}{2}\frac{m^* e^2}{\varepsilon_0 \hbar} N_{eff}$$

where $N_{eff} = N_s + (32/11)N_{dep}$, N_s is the electron density in the well, $N_{dep} = N_i^b / W_d$, and W_d is the width of the depletion region in the well-forming semiconductor. For very high purity well-forming semiconductors, the concentration of dopants is very small and therefore very often the term 32/11 N_{dep} can be neglected in comparison with N_s.

In thermal equilibrium the charge transfer across the interface is governed by the condition [25],

$$E_0 + E_F = V_0 - E_b - \frac{4\pi e^2}{2\varepsilon_0}\frac{(N_s + N_{dep})^2}{N_i^r} - \frac{4\pi e^2}{\varepsilon_0}(N_s + N_{dep})\cdot d + \frac{4\pi e^2}{\varepsilon_0} N_s \frac{B'^2}{b'} \quad (9)$$

where E_b is the donor binding energy in the doped region of the barrier-forming semiconductor. For large enough band offsets the last term, representing the charge penetrating the barrier, is very small and can be safely ignored. Eq. (9) has been obtained using the neutrality condition,

$$N_s + N_{dep} + N_i^r(L-d) \quad (10)$$

where L – d is the depletion width of the intentionally doped region of the barrier.

2.2 *Electronic Structure of p-type MDH*

Transport of a 2D hole gas has been much less extensively studied both theoretically and experimentally. The complex nature of the valence Γ_8 band maxima in group III-V semiconductors makes a detailed analysis of the electronic structure of 2D holes difficult and numerically involved. The main difference in the description of electron and hole electronic structures is that in the case of holes one has to consider the four-fold degenerate valence band. Therefore, the Schrödinger equation (Eq. (4)) is replaced by,

$$\left[H\left(\vec{k}, \frac{1}{i}\frac{\partial}{\partial z}\right) + V(z)\right] \chi_{nk}(z) = E_{nk(z)} \quad (11)$$

where H is a 4x4 $\vec{k}\cdot\vec{p}$ matrix with k_z replaced by the operator $\partial/i\partial z$, V (z) is the potential including band offsets and electrostatic interactions with charged impurities. Eq. (11) has to be solved for each pair of (k_x,k_y).

Numerical calculations of the band structure for specific p-type MDHs have been performed by several groups [29-31]. The main conclusion of these calculations was that the electronic structure of the four-fold degenerate Γ_8 valence band splits into a number of subbands. For $k_x=k_y=0$ these subbands are two-fold spin degenerate. Also, as is shown in Fig. 2, for the case of a p-type AlGaAs/GaAs MDH, the energy dispersion relations for the light and heavy holes are described by nonparabolic energy dependent effective masses [31]. Also, it has been demonstrated that the constant energy surfaces are warped, therefore the effective masses depend on a crystallographic direction. A detailed description of the hole transport in such systems would require extensive numerical calculations. However, under certain conditions, one can use an approximation which can significantly simplify the problem. As is seen in

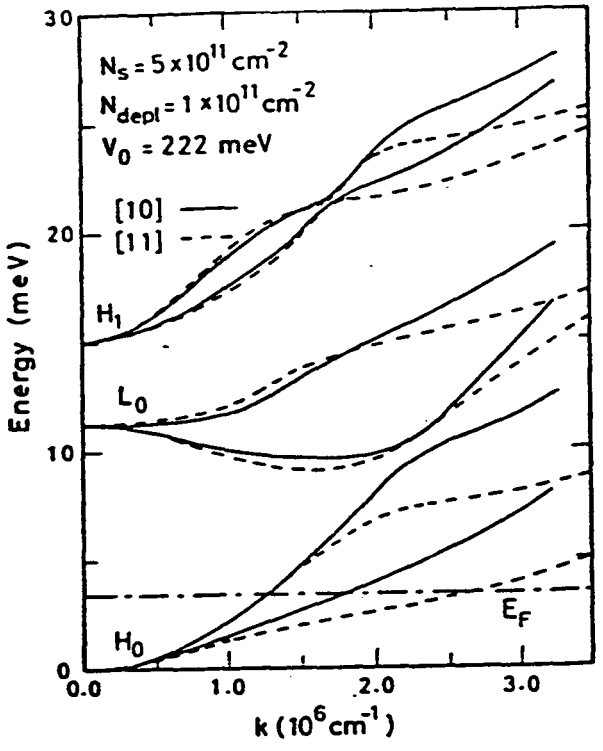

Fig. 2:Calculated hole subband energies of p-type AlGaAs/GaAs MDH as functions of the k wavevector for two different directions, [10] and [11]. Note that the sign of the hole energy is reversed. (After ref. [31])

Fig. 2, the first excited subband is located at about 10 meV below the ground subband. Therefore, for all practically achievable hole concentrations, the Fermi energy is low enough so that only the ground subbands are occupied. Consequently, at low temperatures one has to consider transport within the ground spin-up and spin-down subbands only. Under such approximations one can use an approach previously described for electrons in n-type MDHs. Therefore, we can write the hole wave function in the form [32],

$$\chi_h(z) = \left(\frac{b_h^3}{2}\right)^{1/2} z \exp\left(-b_h z/2\right) \qquad (12)$$

where

$$b_h^3 = b_{1h}^3 + b_{2h}^3 \qquad (13)$$

$$b_{ih}^3 = \frac{33\pi e^2}{2\varepsilon_0 \hbar^2} P_i \qquad (14)$$

P_i (i=1,2) is the concentration of holes in spin-up and spin-down subbands, respectively. The wavefunction (12) is used to calculate hole scattering rates for different scattering potentials.

3. CHARGE SCATTERING MECHANISMS IN 2D MDH

Most of the theoretical descriptions of charge transport are based on the solution of the Boltzman equation [4,6,33,34]. For elastic, momentum randomizing scattering processes, the solution of the Boltzman equation can be expressed in terms of an energy dependent relaxation time. For inelastic scattering processes, i.e., the processes in which the electron or hole loses or gains energy comparable or larger than k_BT, a different method to solve the Boltzman equation has to be used. The most frequently used approach is based on either the variational principle [33] or an iterative method used e.g. by Rode [34].

All the major scattering processes limiting the electron and hole mobilities in compound semiconductors are now well established [4,34]. In 3D compound semiconductors the low temperature mobility is determined by ionized impurity scattering and in the case of alloys also by the alloy disorder scattering. In ultra-high purity materials additional contributions from neutral impurities have to be taken into account. With increasing temperature, scattering by phonons comes into play. This scattering mechanism is especially important in lightly doped semiconductors. There are several different ways phonons can scatter charge carriers. The acoustic phonons can scatter electrons or holes via the deformation potential mechanism. Also, since compound semiconductors lack the center of inversion symmetry, the carriers can be scattered by acoustic phonons via the piezoelectric mechanism. Finally, the carriers can be scattered by optical phonons. The major contribution to the scattering of electrons by optical phonons comes from the interaction of electrons with electrostatic Fröhlich potential. In addition to the polar interaction the holes can be scattered by optical phonons via the optical phonon deformation potential.

Among those different scattering mechanisms, only the scattering by ionized impurities and by alloy disorder can be considered as strictly elastic processes. Scattering by phonons always results in an exchange of energy. However, in the case of acoustic phonons the energy of phonons for small phonon wavevectors is very low. Therefore, for all practical purposes the scattering by acoustic phonons can be treated as an elastic process for the temperatures higher than ~4 K. A high wavevector independent optical phonon energy leads to strongly inelastic scattering in the whole, practically important temperature range. It should be noticed, however, that the optical phonon scattering is strongly reduced at low temperatures. Therefore, in most instances this scattering process can be neglected at temperatures below ~40 K.

There are certain features which distinguish electron transport in two and three dimensions. In the case of ionized impurities there are two distinctly different types of scattering in the 2D case: Electrons can be scattered by remote impurities located within the doped region of the S2 semiconductor as well as by residual impurities and/or charged defects in the S1 semiconductor. Also, there is the possibility of charge scattering by structurally rough interfaces.

For elastic scattering processes the electron or hole mobility can be expressed in terms of energy dependent relaxation times. In general, the total relaxation time is given by the expression,

$$\frac{1}{\tau_{tot}(E)} = \sum_i \frac{1}{\tau_i(E)} \qquad (15)$$

where τ_i (E) are microscopic relaxation times associated with the different scattering processes. The macroscopic relaxation time, and thus also macroscopic mobility, is given by averaging of Eq. (15) over the energy E.

$$\overline{\tau(E)} = \frac{\int \tau(E)\, E\left(\partial f_o / \partial E\right) dE}{\int E\left(\partial f_o / \partial E\right) dE} \qquad (16)$$

where $f_o\,(E) = [1 + \exp\,[(E - E_F) / k_B T]^{-1}$ is the Fermi-Dirac distribution function and E_F is the Fermi energy. In many instances Eq. (16) can be significantly simplified. At low temperatures, when the electron or hole gases are degenerate, $E_F > k_B T$, one has to consider only the electrons or holes on the Fermi surface, and the integration in (16) gives a simple result,

$$\overline{\tau(E)} \equiv \tau\left(E_F\right) \qquad (17)$$

For example, in the case of n-type AlGaAs/GaAs, MDH with $N_S = 3\times10^{11}$ cm^{-2} the condition $k_B T < E_F$ is satisfied for $T < 70$ K. However, for very lightly doped heterostructures or for p-type MDHs with larger effective masses the degeneracy condition is satisfied at much lower temperatures and therefore a numerical evaluation of expression (16) is necessary.

3.1. Scattering by charged centers

Although the objective of modulation doping is to reduce the scattering from Coulomb potentials associated with ionized impurities, nevertheless, the scattering by remote impurities in the barrier and residual background impurities and defects in the well still play a major role in limiting the electron or hole mobilities at low temperatures. The relaxation time for the scattering of charge carriers from a Coulomb potential is given by [9,25],

$$\tau_C^{-1} = \frac{2\pi}{\hbar} \int dz\, N_i(z) \sum_q \left[\frac{2\pi e^2}{q\,\varepsilon(q)}\right]^2 \left|F_C(q, z)\right|^2 \times (1 - \cos\theta)\, \delta\left(E_{\vec{k}} - E_{\vec{k}-\vec{q}}\right) \qquad (18)$$

where $q = 2k \sin(\theta/2)$, θ is the scattering angle, $\varepsilon\,(q)$ is the static dielectric function,

$$\varepsilon(q) = 1 + \frac{2e^2 m^*}{\varepsilon_0 q \hbar^2} F(q) \qquad (19)$$

and ε_0 is the static dielectric constant. The form factors are given by,

$$F_C(q,z) = \int dz' \left|\chi_0(z')\right|^2 \exp\left(-q|z - z'|\right) \qquad (20)$$

and

$$F(q) = \int dz' \int dz' \left|\chi_0(z)\right|^2 \left|\chi_0(z')\right|^2 \exp\left(-q|z - z'|\right) \qquad (21)$$

Expression (19) for the static dielectric function is valid only for T = 0. At $T \neq 0$ a more complex equation including the polarizability of 2D gas at finite temperatures has to be included. A simple expression for the temperature dependent dielectric function has been obtained and used to calculate the mobility in AlGaAs/GaAs MDHs [26],

$$\varepsilon(q) = \left[1 + \frac{q_s}{q}\right] \tag{22}$$

where

$$q_s = \frac{2\pi e^2}{\varepsilon_0} \frac{Ns}{k_B T} \left\{\left[1 + \exp\left(-E_F / k_B T\right)\right] \ln\left[1 + \exp\left(E_F / k_B T\right)\right]\right\}^{-1} \tag{23}$$

An inspection of Eqs. (18) and (20) provides an insight into how the remote impurity scattering is reduced by the separation of the impurities from the quantum well. For the impurities located in the $z' < -d$ region of the barrier and for 2D gas located at z=0 the scattering rate is reduced by an exponential factor $\exp(-2k_F d)$. Therefore, for typical Fermi wavevectors of 10^6 cm^{-1}, a large enhancement of the remote impurity mobility is expected for $d > 10^{-6}$ cm.

3.2. Acoustic phonon scattering

An acoustic wave propagating in a crystal can couple to electrons and holes by deforming the crystal and affecting the positions of the conduction and valence band edges. In binary, partly ionic compounds an additional coupling between acoustic phonons and the carriers stems from the piezoelectric effect produced by the deformation of the unit cell. Both deformation potential and piezoelectric coupling of charge carriers to acoustic phonons are well known and were extensively studied in 3D compound semiconductors [4].

In 2D MDHs it is customarily assumed that the phonons can freely propagate in all directions. Therefore one considers a confined electron or hole gas which interacts with phonons which are 3D in nature [35-41]. Under such assumptions the relaxation times due to deformation potential and piezoelectric acoustic phonon scattering are given by [40],

$$\tau_{DP}^{-1} = \frac{3 m_e^* a_c^2 b_0 k_B T}{16 \pi \hbar^3 C_l} \int_0^{\pi} S^2 (1 - \cos\theta)\, d\theta \tag{24}$$

and

$$\tau_{PE}^{-1} = \tau_L^{-1} + 2\tau_T^{-1} \tag{25}$$

where

$$\tau_{L,T}^{-1} = \frac{\hbar \alpha_{L,T}}{k_B T k^2} \int q S^2 f_{L,T}(q)\, d\theta \tag{26}$$

The screening factor S has the form,

$$S^2 = \frac{q^2}{(q + q_s H)^2} \tag{27}$$

where

$$H = \frac{1 + 9/8\, r + 3/8\, r^2}{(1+r)^3}, \; r = \frac{q}{b_0} \tag{28}$$

a_c is the deformation potential constant and c_l is the elastic constant. The functions $f_{L,T}(Q)$ and constants $\alpha_{L,T}$ are given in ref. [40]. The factor S in Eqs. (24) and (26) represents the screening by free electrons. When the screening is neglected for the short range deformation potential coupling, one obtains the following simple result,

$$\tau_{DP}^{-1} = \frac{3\, m_e^* a_c^2 k_B T\, b_0}{16\, C_l \hbar^3} \tag{29}$$

From this expression one finds that the electron mobility is inversely proportional to the temperature T and the parameter b_0. Therefore, for the deformation potential limited mobility one expects a very weak dependence on the electron density,

$$\tau_{DP} \sim b_0^{-1} \sim \left(N_S + \frac{32}{11} N_{dep}\right)^{-1/3} \tag{30}$$

The piezoelectric coupling limited mobility shows a more complex dependence on the electron density. However, in most instances the deformation potential is the predominant scattering process which determines the total acoustic phonon scattering.

The expressions (24) and (26) were obtained under the assumption that the thermal energy $k_B T$ is larger than the energy of acoustic phonons participating in the scattering process, $k_B T > \hbar\omega_q$. Under such conditions the phonon distribution function can be approximated by,

$$N_q = \frac{1}{\exp\left(\frac{\hbar\omega_q}{k_B T}\right) - 1} \simeq \frac{k_B T}{\hbar\omega_q} \tag{31}$$

At low temperatures this equipartition condition is not satisfied. Also, at such low temperatures the scattering by acoustic phonons cannot be treated as an elastic process. This temperature range corresponds to the so-called Bloch - Grüneisen (B-G) regime. [42,43]. Theoretical studies have shown that in this regime the acoustic phonon mobility is very rapidly increasing with decreasing temperature [43,44]. Recently, a strong increase of the acoustic phonon limited

mobility has been experimentally observed by subtracting the temperature independent part of the electron mobility in high quality AlGaAs/GaAs MDHs [43]. It should be noted, however, that at very low temperatures the scattering by charged centers is the dominant process limiting electron and hole mobilities and that the B-G regime cannot be clearly distinguished from direct measurements of the electron or hole mobilities.

3.3. Optical phonon scattering

A proper treatment of optical phonon scattering is by far the most complex problem of charge transport in 2D systems. The large optical phonon energy (30 meV to 40 meV) makes the scattering process highly inelastic even at room temperature. In addition, since the typical energy separation between electric subbands is of the order of 10 meV, an optical phonon can couple several subbands. Any theoretical treatment of this problem requires an accurate knowledge of the energies and wave-functions for all those subbands [45]. Numerical calculation of the optical phonon scattering rates for AlGaAs/GaAs MDH have shown that although the 2D confinement leads to reduction of the optical phonon mobility at 77 K, the room temperature mobilities in the 2D and 3D cases are practically the same [45]. This finding is consistent with the experimental results which demonstrated that the optical phonon limited mobility does not depend on the size of the 2D confinement or on the density of 2D electrons [46].

These results provide justification for another approach proposed in Ref. (26) where it has been argued that since the optical phonons probe a wide range of subbands, therefore, the density of states participating in transport is an average over all those subbands. It can be shown that the total density of states for several subbands resemble the density of state of 3D gas. Consequently, one can use a 3D approximation to calculate the optical phonon scattering in 2D MDHs.

3.4. Alloy disorder scattering

For MDH involving ternary compounds, an additional scattering from random alloy-disorder potential has to be included [47]. Two distinctly different types of MDHs containing ternary compounds are possible [48,26]. In the first one the well is formed by a binary compound and the barrier is formed by a ternary alloy. In such MDH there is no significant alloy scattering. The only contribution to this scattering process is through the scattering of the charge carriers penetrating into the barrier. In the other type of structure with the well formed by the ternary alloy the charge carriers are very efficiently scattered by the disordered alloy in the well.

Since the alloy disorder scattering results from a potential, localized to within one unit cell, there is a formal similarity between this scattering

mechanism and the deformation potential, acoustic phonon scattering. In the case of the quantum well formed by the ternary compound the relaxation time is given by Eq. (24) with $a_c^2 k_B T/C_l$ replaced with $x(1-x)\Omega\langle V\rangle^2$ where x is the alloy composition, Ω is the unit cell volume and $\langle V\rangle$ is the alloy disorder parameter. In order to evaluate the carrier mobility for 2D gas confined within the binary semiconductor, the scattering rate has to be reduced by the additional factor [26],

$$\frac{64\pi^2 e^4 \hbar (N_s/2 + N_{dep})^2}{3\varepsilon_0^2 (2m^*)^{1/2} V_0^{5/2} b_0} \tag{32}$$

For a very large band offset, V_0, the penetration of the wavefunction into the barrier is very small and, as is seen from Eq. (32), the contribution of alloy-disorder scattering is very low.

3.5. Interface roughness scattering

Despite the atomic scale precision of the modern epitaxial growth techniques, most of the epitaxially grown interfaces exhibit some degree of structural roughness. A rough interface can scatter the carriers confined in the well. The interface roughness plays a very significant role in scattering of electrons in Si metal-oxide-semiconductor structures [49]. The scattering process is especially significant at higher electron densities. The theoretical expression originally obtained for Si inversion layers [9] has been adopted to 2D gas in MDHs [25],

$$\tau_{IR}^{-1} = \frac{2\pi}{\hbar} \sum_{\bar{q}} \left[\frac{\Delta \Lambda F_{eff}}{\varepsilon(q)}\right]^2 \exp\left(-\frac{1}{4} q^2 \Lambda^2\right) \times (1-\cos\theta)\, \delta\left(E_{\bar{k}} - E_{\bar{k}-\bar{q}}\right) \tag{33}$$

Here, Δ represents the mean square deviation of the height and Λ is a measurement of the lateral spatial decay rate of the roughness, respectively. The effective field is given by

$$F_{eff} = \frac{4\pi e^2}{\varepsilon_0}\left(\frac{1}{2} N_s + N_{dep}\right) \tag{34}$$

One finds from Eq. (33) that the interface-roughness scattering rate is greatly reduced for Λ greater than the carrier wavelength, $2\pi/k_F$. This can be contrasted with the case of nonspecular scattering of a quasi-3D electron gas in wide-parabolic quantum wells [50], where the largest contribution comes from large size fluctuations. The interface-roughness has been frequently invoked to explain lower than usual mobilities in MDHs [51,52]. However, since there is no independent way to measure the parameters Δ and Λ, it is difficult to ascertain the relative importance of this scattering compared with the other low temperature scattering processes.

3.6. Intersubband scattering

All the above considerations of the elastic scattering process were restricted to the case of carrier transport within a ground electric subband. This approximation is strictly applicable only to the transport at low temperatures and low carrier densities when only the lowest subband is occupied. In heavily doped MDHs one has to account for the occupation of higher lying subbands [45, 53]. A proper treatment of multisubband transport is difficult since one has to consider the momentum randomizing events within all occupied subbands, as well as the scattering between the subbands. Such a problem, in general, requires solving of a set of coupled Boltzman equations which can be done only numerically. Numerical solutions of multisubband transport was presented in Refs. [45, 53, 54].

In Ref. [26] a simplified approach to the transport in the two lowest subbands has been proposed. Instead of solving two coupled Boltzman equations it has been assumed that since the concentration and momentum of the carriers in the upper subband is much smaller than those in the ground subband, therefore, one can neglect the contribution of the upper subband to the total conductivity. The only effect of this subband is that it provides additional channel for the carrier scattering. Since there is a large momentum change for the carriers which are scattered from the ground to the excited subband, therefore, such scattering processes will lead to a substantial reduction of mobility of the carriers. The intersubband scattering rates for various scattering potentials were derived in Ref. [26] and were used to calculate scattering rates in AlGaAs/GaAs and InAlAs/InGaAs MDHs.

3.7. Scattering mechanisms in p-type MDH

As has been discussed in Section 2, the transport of holes in p-type MDHs has attracted much less attention. The available experimental data is restricted to AlGaAs/GaAs MDHs [23,55-57]. Also, the only existing theoretical treatment of the 2D hole transport is limited to a simple approach proposed by the present author and based on the assumption of decoupled spin-up and spin-down subbands [32,38,58]. It has been argued that since the light holes in the spin-down subband are very efficiently scattered by the heavy holes in spin-up subband, the mobility of holes in spin-down states is much lower. This, combined with a much smaller concentration of light holes in spin-down band , provides justification for neglecting the light hole contribution to the total conductivity. Under such circumstances the mobility of a 2D hole gas can be described in terms of carrier transport in a single subband. This allows use of the methods previously developed for a single parabolic electronic subband with one important modification which takes into account the p-type symmetry of the valence band Bloch wavefunctions. The scattering rates for long range

interactions (Coulomb and piezoelectric acoustic phonon scatterings) given by Eqs. (18) and (26) have to be multiplied by a factor of $1/4(1+3\cos^2\theta)$.

In the case of the deformation potential interaction the deformation potential constant a_c in Eq. (24) is replaced by an effective valence band deformation potential, E_{dp}, which has been shown to have the form [38],

$$E_{dp}^2 = E_{intra}^2 + E_{inter}^2 \tag{35}$$

where

$$E_{intra}^2 = \frac{C_l + C_t}{4C_L}\left[(l+m)^2 + n^2\right] + \frac{C_l}{4C_t}m^2 \tag{36}$$

and

$$E_{inter}^2 = \frac{m_2^*}{3m_1^*}\frac{C_l}{C_t}m^2 \tag{37}$$

represent intra and inter subband scattering, respectively, C_t is the transverse elastic constant, m_1^* and m_2^* are heavy (spin-up) and light (spin-down) hole effective masses, and l, m and n are the valence band deformation potential parameters [59].

As is shown in section 3.4., the strength of the alloy-disorder scattering is determined by the parameter, $\langle V\rangle$. For the conduction band electrons $\langle V\rangle = \langle S|V|S\rangle$ where $\langle S|$ is the conduction band Bloch amplitude and V is the difference of the core potentials of two elements in the alloy. For the valence band hole the alloy-disorder parameter $\langle V\rangle$ is replaced by $\langle V_v\rangle$, given by,

$$\langle V_v\rangle = \langle X|V|X\rangle \tag{38}$$

where X is the Bloch amplitude for the Γ_8 valence band. The parameters $\langle V\rangle$ and $\langle V_v\rangle$ can be related to the conduction band and valence band offsets for the binary compounds forming the alloy.

4. SCATTERING MECHANISMS IN WIDE PARABOLIC WELLS

So far we have considered 2D systems in which charge carriers are confined in one direction, and can freely move in a 2D plane. Such systems satisfy both conditions (1) and (2), necessary for a fully quantized 2D motion of the charge. Also, modulation (or remote) doping allows for a dramatic reduction of ionized impurity scattering. In standard 3D structures the ionized impurities and charge carriers are not spatially separated and ionized impurity scattering is the dominant process limiting the mobility at low temperatures.

Recent progress in the epitaxial growth of AlGaAs films allowed a realization of a new type of structure which has all the basic features of 3D

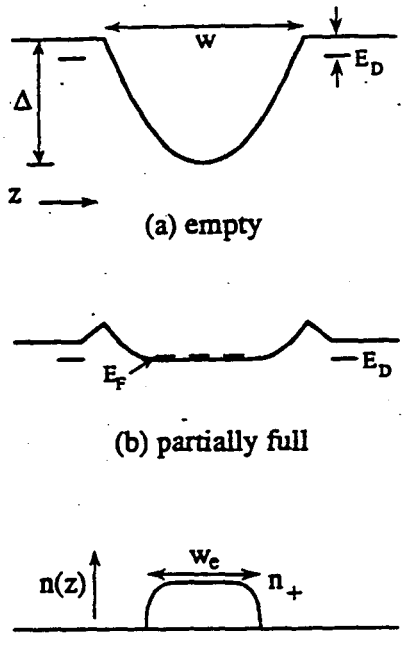

Fig. 3:Schematic illustration of the conduction-band edge in (a) an empty parabolic well, (b) a partially full well. The electron density profile is shown in (c). (After ref [60]).

systems and still has impurities removed from the immediate vicinity of the charge carriers [19,20]. In modulation (or remotely) doped wide parabolic wells the composition of $Al_xGa_{1-x}As$ in the well is parabolically varied with the distance. As shown in Fig. 3, for the case n-type AlGaAs/GaAs structure, this creates a well with the conduction band edge parabolically dependent on the distance [60]. If such a structure is doped in the regions outside the well, the electrons are transferred to the well. The resulting electrostatic potential flattens the bottom of the well. Consequently, one obtains a structure in which electrons are confined in a wide well and are separated from their parent donors. This design allows preparation of wells with a thickness of the order of 1000 Å and with the electron concentration of about 10^{16} cm^{-3} [60].

From condition (1) we find that the de Broglie wavelength of the electron gas in such systems is smaller than the well width. Therefore, the electron motion in the well is not quantized. Such system can be considered a model of modulation doped 3D electron gas, which should exhibit an enhanced low temperature electron mobility. In fact, mobilities as high as 3×10^5 $cm^2/V\cdot s$ were observed in AlGaAs/GaAs wide parabolic wells [50]. Although such mobilities are much higher than those observed in standard 3D semiconductors, they are still much lower than mobilities in 2D MDH or what one would expect in any modulation doped system.

The reason for this lower than expected mobility lies in nonspecular scattering of the electrons from rough confinement walls. As has been discussed in Section 1, in addition to the condition (1), one also has to consider condition (2), which in general is less restrictive than Eq. (2), and is easily satisfied in 2D MDHs. In wide parabolic wells with $\simeq 3\times10^5$ $cm^2/V\cdot s$ and $n \simeq 3\times10^{16}$ $cm^{-3}/V\cdot s$,

$$l_p \simeq 10^4 \text{ Å} > w_e = 10^3 \text{ Å}$$

This means that although the electron motion is not quantized in the parabolic well the mean free path of the electron is much larger than the well width. The transport of electrons in the well will be affected by the interaction with the confining walls.

The conditions resemble the situation frequently observed in thin metallic films characterized by a small de Broglie wavelength and high electron mobility.

The interaction of the electrons with the confinement walls reduces the electron conductivity in the plane of the well. This effect was extensively studied in metals and is known as the size effect in thin metallic films [61,62]. The effects of electron interaction with the confinement walls in wide parabolic wells has been considered in Ref. [50]. Adopting the approach previously developed for thin metallic films [63], it can be shown that the conductivity in parabolic wells is given by,

$$\sigma = \frac{3\sigma_b}{4}\int_0^{\pi} d\theta \frac{\sin^3(\theta)}{1+{l_b}/{l_s(\theta)}} \tag{40}$$

where $\sigma_b = ne\mu_b$ is the bulk conductivity, l_b is the bulk mean free path, $l_s(\theta)$ is the effective electron mean free path associated with electron scattering from the confining wells, and θ is the angle of incidence at a wall. It was shown that [63],

$$l_s(\theta) = -w_e/\{|\cos(\theta)|\ln[p(\theta)]\} \tag{41}$$

where $p(\theta)$ is the specularity parameter representing the probability that an electron will be specularly reflected from a wall, and w_e is the well width.

For randomly rough walls the specularity parameter takes the form [64],

$$p(\theta) = \exp\left[-\left[\frac{4\pi\alpha}{\lambda}\right]^2 \cos^2\theta\right] \tag{42}$$

where α is the roughness parameter, and λ is the electron wavelength. It has been argued that the parameter α should be of the order of Thomas-Fermi screening length [50],

$$\alpha = R_s = \left(\frac{2\sqrt{2}\,e^2 m^{*3/2}(k_B T)^{1/2}}{\pi\hbar^3\varepsilon_0} F_{-1/2}\left({E_F}/{k_B T}\right)\right)^{-1/2} \tag{43}$$

where $F_{-1/2}(\cdot)$ is the Fermi-Dirac integral of the order $-1/2$. Substitution of Eqs. (41) and (42) into Eq. (40), and integration over θ yields an analytic expression for the electron mobility in the parabolic quantum well,

$$\mu = \mu_b G(c) \tag{44}$$

where

$$G(c) = c^{-1/3}\frac{1}{4}\ln\left[\frac{\left(1+c^{1/3}\right)^3}{(1+c)}\right] = \frac{\sqrt{3}}{2}\left[\tan^{-1}\left[\frac{2c^{1/3}-1}{\sqrt{3}}\right]+\frac{\pi}{6}\right] \qquad (45)$$

where $c = 4\, l_b\, k_F^2\, \alpha^2 / w_e$. For perfectly smooth walls $\alpha \rightarrow 0$ or for a very wide well $w_e \rightarrow \infty$, $c \rightarrow 0$ and, as expected, $\mu \rightarrow \mu_b$.

5. CALCULATED MOBILITY AND COMPARISON WITH EXPERIMENT

Lattice matching at heterointerfaces is one of the principal requirements to achieve high quality, high mobility MDHs. To date the $Al_xGa_{1-x}As/GaAs$ heterointerface is the system most often used to fabricate MDHs. Since AlAs is quite well lattice matched to GaAs, therefore, there is the possibility of preparing MDHs with variable composition of Al in AlGaAs barriers. This adds a degree of freedom in creating MDHs with variable band offsets or to taylor the barrier height for specific applications. Other possible lattice matched systems do not offer such flexibility. For example, $In_xGa_{1-x}As$ is lattice matched to InP only for $x = 0.53$. Also, $In_yAl_{1-y}As$ is lattice matched to either InP or $In_{0.53}Ga_{0.47}As$ only for $y = 0.48$. Recently, there has been significant progress in improving the quality of the lattice mismatched pseudomorphic hetero-systems. However, the electron or hole mobilities in strained systems are still much lower than those in the lattice matched MDHs [14].

In this section we shall present results of calculations of electron and hole mobilities in various MDHs and in wide parabolic wells. The results will be compared with existing experimental data. We will also discuss several aspects of carrier transport in artificially structured systems which are still controversial and not fully understood. Here we present results of calculations of electron mobility in MDHs in which the electron gas is confined in GaAs or in $In_{0.53}Ga_{0.47}As$ with the barrier formed by either AlGaAs, in the former, or by InP or $In_{0.48}Al_{0.52}As$ in the latter case.

5.1. N-type $Al_xGa_{1-x}As/GaAs$ MDH

The parameters describing the band structure of $Al_xGa_{1-x}As/GaAs$ MDHs, along with the coupling parameters for electron-phonon interactions, are known from studies of electron transport in bulk GaAs. Here we adopt the parameters listed in Ref. [38]. We also assume a value of 0.26 eV for the conduction band offset at the $Al_{0.35}Ga_{0.65}As/GaAs$ interface and a value of $\langle V \rangle = 0.5$ eV for the alloy disorder parameter in AlGaAs. This value of $\langle V \rangle$ is smaller than the previously used $\langle V \rangle = 1$ eV [25,26]. However, it should be

pointed out that the alloy disorder scattering contribution to the total scattering is negligibly small with the possible exception of the MDHs with high 2D electron densities, approaching 10^{12} cm^{-2} [26].

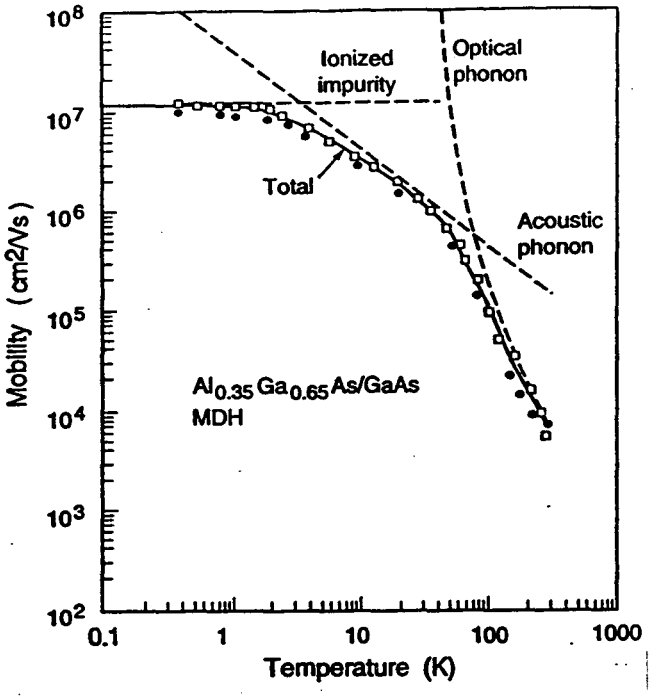

Fig. 4:Theoretical temperature dependence of the electron mobility in AlGaAs/GaAs MDH with a spacer width of 700 Å. Points are experimental data of ref. [21] (□) and ref. [22] (•) for the spacer width 700 Å and 750 Å, respectively.

The calculated temperature dependence of the electron mobility in $Al_{0.3}Ga_{0.7}As$/GaAs MDH is shown in Fig. 4. Comparison of these calculations with available experimental data [21,22] on high quality MDHs indicates that in the wide temperature range of 4 K to 300 K the electron mobility is determined by phonon scattering. The optical phonons dominate at $T > 70$ K and the acoustic phonon scattering plays a major role in the range 4 K to 40 K. At even lower temperatures the mobility levels off due to the scattering from remote impurities in the barrier and residual impurities or charged defects in nominally undoped quantum wells. The alloy disorder scattering of the electrons penetrating the AlGaAs barrier is very small and amounts to about 4% of the total scattering in MDHs with an electron mobility of 10^7 cm^2/V•s.

The mobility in Fig. 4 has been obtained assuming the equipartition condition for the acoustic phonons. As has been shown previously [43] this condition is valid only for $T \gtrsim 4$ K. At lower temperatures the acoustic phonon mobility drastically increases with decreasing temperature, $\mu_{ac} \sim T^{-s}$, where the exponent s depends on the type of coupling. Mobility calculations in the B-G regime show that s=5 for piezoelectric scattering [43]. Also, it has been found that for the screened deformation potential, s=7, whereas it is reduced to s=5 when the screening is not included [43]. As is seen in Fig. 4, the B-G regime cannot be clearly observed in the experimental data because of the onset of temperature independent scattering from charged centers.

The electron mobility due to optical phonons was calculated using the 3D approximation [26]. The justification for the approximation has been discussed in Section 4.4. It is also seen in Fig. 4 that this approximation quite well describes the 2D electron mobility for $T > 100$ K, supporting the conclusion

about insensitivity of optical phonon scattering to electron gas confinement [46]. Since the ionized impurity scattering contributes only at low temperatures where the 2D electron gas is degenerate, the mobility due to this scattering is independent of the temperature for $T < 40$ K. In high-quality MDHs the ionized impurity mobility is temperature dependent only at higher temperatures where the ionized impurity contribution to the total scattering is insignificant.

The calculated total mobility in Fig. 4 has been obtained using the Matthiessen's rule, i.e., instead of averaging the total microscopic relaxation time over energy using equation (15), one performs the averaging for each of the scattering mechanisms separately and then combines all the relaxation times to obtain the total mobility. Using both methods we find that for the MDH shown in Fig. 4, the error of using Matthiessen's rule does not exceed a few percent.

As seen in Fig. 4, simple model calculations account extremely well for the temperature dependence of the electron mobility in high-quality AlGaAs/GaAs MDHs. In the structures reported in Refs. [21] and [22] the low temperature mobility exceeds 10^7 cm^2/V • s and is mostly determined by scattering from remote impurities. In the MDH measured in Ref. [22] with a spacer width of 750 Å additional scattering from the background impurities with concentrations of only 2×10^{13} cm^{-3} is required to account for the maximum mobility of 1.05×10^7 cm^2/V•s.

The early studies of AlGaAs/GaAs MDH have demonstrated that the mobility of 2D electrons depends on the growth sequence of the epitaxial layers forming the heterostructure [65]. The very high mobilities can be achieved only in so-called normal-MDH (N-MDH) in which high purity well-forming GaAs is grown first, followed by the growth of the barrier forming, doped AlGaAs. In an inverted-MDHs (I-MDH) in which the growth sequence is reversed the mobilities are typically about one order of magnitude lower than in a normal MDH.

Several explanations have been put forward to understand the reduced mobility in I-MDHs. It has been proposed that the inverted heterointerfaces are less structurally perfect [65]. These imperfections would scatter the electrons resulting in lower mobility [65]. It has also been suggested that a diffusion of impurities from heavily doped regions in AlGaAs towards the well can be responsible for an increased ionized impurity scattering [66].

Most recently a new explanation for the mobility reduction in I-MDH has been advanced [67]. It has been shown that there is a significant difference in the native defect incorporation in I- and N-MDHs. In I-MDH the well-forming GaAs layer is grown in the presence of electrons transferred from heavily doped barriers forming AlGaAs. The electrons enhance the incorporation of native charged defects [68]. These defects act as scattering centers reducing the electron mobility in the well. The effect of scattering by the charged defects in the well of a typical AlGaAs/GaAs I-MDH is shown in Fig. 5. The electron mobility is found to be at least one order of magnitude lower than that expected in an

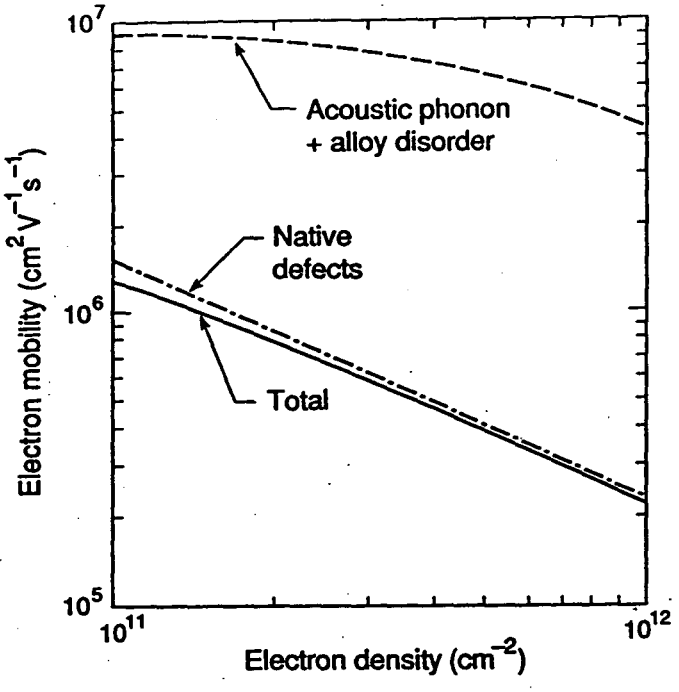

Fig. 5:Electron mobility as a function of 2D electron gas density in inverted AlGaAs/GaAs MDH at 4K. The native defect scattering is the dominant mechanism limiting the mobility.

equivalent N-MDH. The proposed explanation is supported by studies which indicate that a long range Coulomb potential, rather than short range interface roughness, is responsible for the low mobilities observed in I-MDHs [69].

In most high-quality MDHs, the 2D electron density is very low when the structure is measured in the dark. However, one can increase the density by illumination of heavily doped AlGaAs with infrared light of energy ~ 1 eV [70]. The illumination transfers the deep DX-like donors into a shallow donor configuration leading to much more efficient charge transfer to the well. A typical light induced 2D density is ~ 2×10^{11} cm^{-2} to 3×10^{11} cm^{-2} [21,22]. It has been also shown that the concentration of electrons can be controlled with an external electric field applied to the backside of MDH [71]. By increasing the electron density one can reach conditions where the higher lying excited subbands are occupied. Experimental results indicate that the onset of the occupation of the first excited subband is always associated with a decrease of the measured electron mobility. Systematic studies have shown that in AlGaAs/GaAs MDH, the mobility decreases by about 30% when the first excited subband is occupied [71,73]. Simple theoretical calculations in Ref. [26] are consistent with these results. It has been found that the onset of the intersubband scattering reduces the electron mobility due to acoustic phonons and background ionized impurities by about 28%. It has been also shown that the remote ionized impurities contribute very little to the intersubband scattering due to an exponential reduction of the scattering rates at large momentum transfers.

5.2. N-type $In_{0.53}Ga_{0.47}As$ based heterostructures

In InP/InGaAs and InAlAs/InGaAs MDHs the well-forming $In_xGa_{1-x}As$ is lattice matched to InP and InAlAs for x=0.53. There is one important difference between the charge transport in GaAs and in InGaAs. In the latter case the

electrons are very efficiently scattered by the alloy-disorder potential in the well. Early experimental results on the 2D electron gas mobilities have shown that the mobility is independent of temperature for $T < 50$ K [74]. Also, the highest reported mobilities were limited to about 10^5 cm^2/V•s. These results were confirmed on both InAlAs/InGaAs [75] and on InP/InGaAs [76] MDHs.

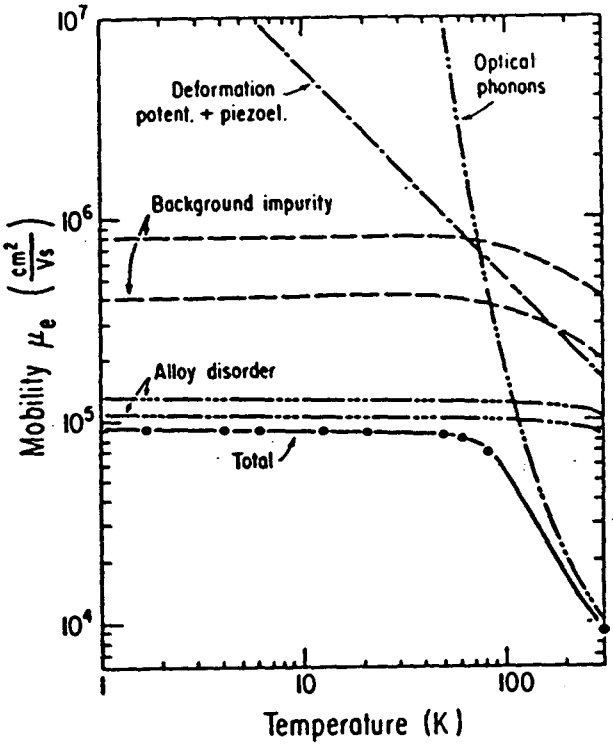

Fig. 6:Electron mobility vs. temperature in $In_{0.48}Al_{0.52}As/In_{0.53}Ga_{0.47}As$ MDH with 80 Å spacer. Experimental points are from ref. [74]. The upper and lower background impurity mobilities correspond to $N_i^b = 5\times10^{15}$ cm^{-3} and 10^{16} cm^{-3}, respectively. Alloy disorder potential $\langle V \rangle$ was used as a fitting parameter. (After ref. 26)

Theoretical calculations have demonstrated that the mobility at these low temperatures is determined by alloy disorder scattering in the well [26,48,77]. Fig. 6 shows the comparison of the theoretical calculation with the experimental data of Ref. [74]. The material parameters used in the calculations are given in Ref. [26]. Because of high electron density in the MDH studied [74], the calculations included the effects of the first excited subband using the approximate approach outlined in Section 3.6. An analysis of the low temperature mobility data was used to determine the alloy-disorder parameter $\langle V \rangle$. It has been found that the experimental results can be explained assuming $\langle V \rangle$ to be in the range of 0.55 eV to 0.63 eV. This value very favorably compares with the independent determination of $\langle V \rangle = 0.6$ eV reported in Ref. [78].

5.3. P-type AlGaAs/GaAs MDH

As has been discussed in Section 3.7, there is only a very limited amount of experimental data on transport properties of 2D holes in MDHs. Practically all of the data is restricted to the AlGaAs/GaAs system [23,55,56]. Similarly, as in the case of electrons, modulation doping leads to a large increase of the 2D hole mobilities. A low temperature mobility as high as 3.8×10^5 cm^2/V•s was measured at $T = 0.3$ K [23]. The only theoretical calculations of the 2D hole

mobilities are based on the model of decoupled electric subbands [32,38,58]. It has been shown in these calculations that only the heavy holes contribute significantly to the total conductivity in a MDH. The contribution of the light holes is much smaller since they are very efficiently scattered by the heavy holes. Therefore, the transport in p-type MDHs can be described in terms of single heavy hole electric subband. Theoretical calculations of the hole mobility in a p-type AlGaAs/GaAs MDH with the hole density of 2×10^{11} cm^{-2} are shown in Fig. 7 [58]. Very good agreement between the calculated mobility and the experimental data of Ref. [57] is obtained. In the temperature range 4 K to 80 K the mobility is determined by phonon scattering. The largest contribution to the scattering is coming from the acoustic phonon scattering which is the dominant scattering mechanisms up to the temperature of ~ 60 K. The discrepancy between theory and experiment for T < 4 K can be attributed to the background ionized impurity scattering. This scattering mechanism has not been included in the calculations.

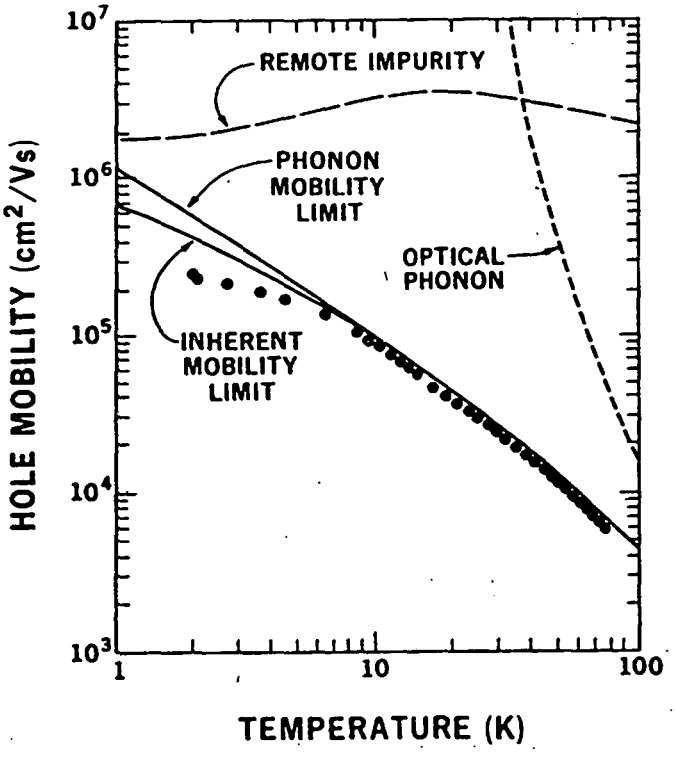

Fig. 7:Temperature dependent hole mobility in p-type $Al_{0.5}Ga_{0.5}As$/GaAs MDH. The points represent experimental data of ref. [57] for the hole density P = 2×10^{11} cm^{-2}. (After ref.[58])

The theoretical results in Fig. 7 were obtained for an unscreened acoustic phonon deformation potential scattering. This is consistent with the calculations of the electron mobility where the screening of the deformation potential has not been included. The problem of the proper screening of the short range potentials has been discussed in several papers. It has been shown recently that the electron energy loss rates [27], as well as phonon-drag contribution to the thermoelectric power [39] in 2D electron systems, can be explained assuming the unscreened deformation potential. However, it has also been argued by others that the dependence of the phonon scattering on the electron density can be better understood when the screening is included in the calculations [79,80].

It has been found that to explain experimentaly observed mobilities with a screened deformation potential very high values of deformation potential

constants are required. Thus, in AlGaAs/GaAs MDH, deformation potentials as high as 13.5 eV were used to explain the value of the acoustic phonon limited mobility [80]. Such a high value is at variance with the results on electron mobility in high purity GaAs [81] and is much higher than the value of $a_c = -9.3$ eV directly determined by an independent experiment [82]. Also, theoretical calculations has provided even a lower value of $a_c = -7.3$ eV [83].

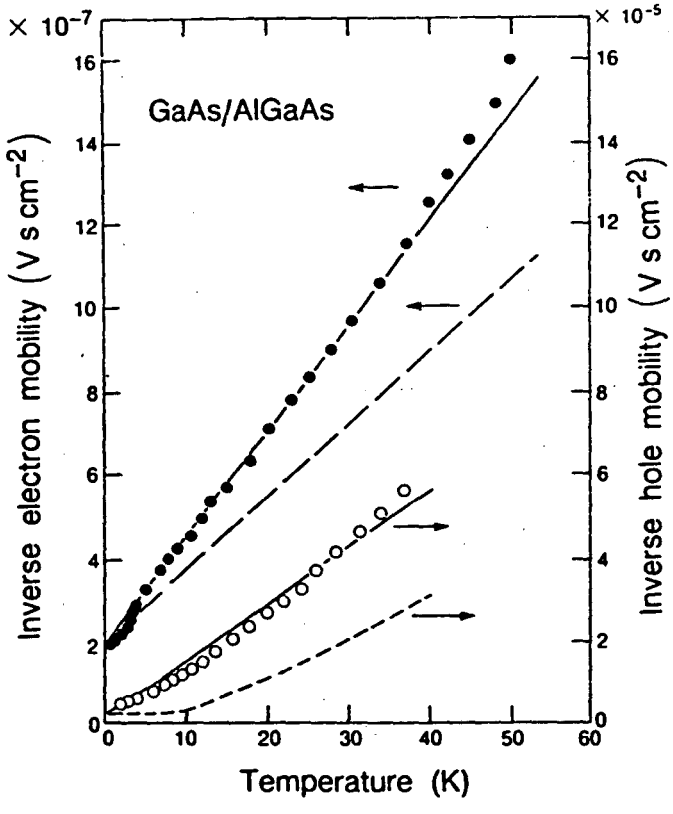

Fig. 8:Temperature dependence of the inverse electron and hole mobilities in AlGaAs/GaAs MDHs. The experimental points are from refs [57]; (o) and ref. [84]; (•). The solid and broken lines represent the calculated mobilities for unscreened and screened deformation potentials, respectively. (After ref. [38])

The analysis of electron and hole mobilities in high quality MDH provides an independent test for the values of the conduction and valence band acoustic phonon deformation potentials [58]. As is shown in Fig. 8, the temperature dependences of inverse electron and hole mobilities are well explained by calculations in which acoustic phonon deformation potential interaction is not screened by free carriers. The best fit is obtained for $a_c = -9.3$ eV and $a_v = -0.7$ eV. These values of the deformation potentials were independently determined from other experiments [82]. It is also seen in Fig. 8 that incorporation of screening very significantly reduces the acoustic phonon scattering rates which are much lower than those determined experimentally. Therefore, the results in Fig. 8 support the notion that a simple Fermi-Thomas screening of the short range deformation potential cannot be used in 2D systems.

5.4. Wide parabolic AlGaAs/GaAs wells

The wide parabolic wells were designed to simulate quasi-3D systems with reduced ionized impurity scattering. It has been proposed that such systems could exhibit Wigner crystallization at very low temperatures. Although the crystallization has not ever been clearly observed, it has been shown that wide-parabolic wells exhibit other interesting and unique properties. It has been demonstrated that the maximum mobility in AlGaAs wells was limited to about 3×10^5 cm^2/Vs. This value of mobility was lower than that expected for a quasi-3D degenerate electron gas. It has been proposed in ref. [50] that the value of electron mobility in wide parabolic wells is affected by nonspecular scattering of electrons from rough confining walls. As has been shown in Section 3, the electron mean free path is larger than the well width. Consequently, the electrons are reflected from the rough walls more often than they interact with scattering centers in the well. In order to calculate the effect of the nonspecular reflection, a model theory which has been previously developed to calculate the size effect in thin metallic films has been adopted to evaluate electron mobility in parabolic wells. Results of the calculations are shown in Fig. 9. The results indicate that the nonspecular scattering reduces the electron mobility by a factor of 2 to 3. It is also seen in Fig. 9 that incorporation of nonspecular scattering accounts for the experimentally observed temperature dependence of the mobility.

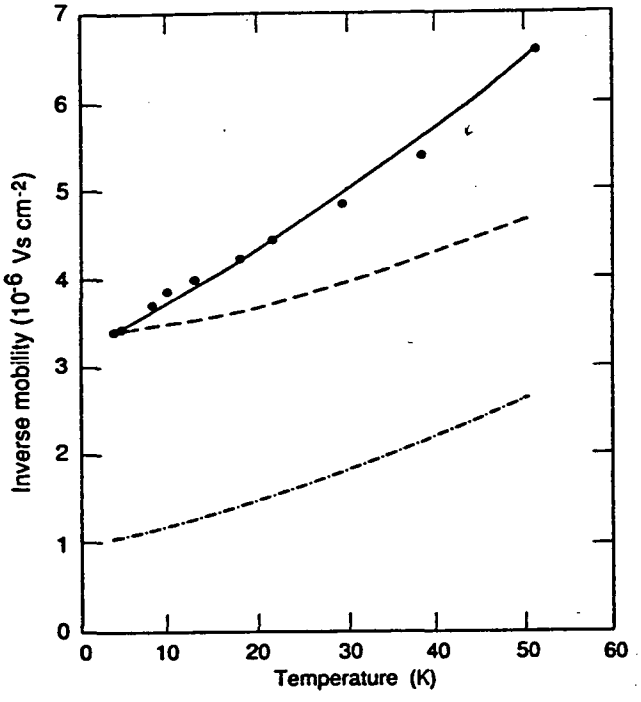

Fig. 9: Temperature-dependent inverse mobility in wide-parabolic AlGaAs/GaAs wells. (___), scattering from rough walls included, ionized impurity concentration $N_i^b = 2.3\times10^{14}$ cm^{-3}; (-·-·-) , no scattering from the walls, $N_i^b = 2.3\times10^{14}$ cm^{-3}; (-----) no scattering from the walls, $N_i^b = 10^{15}$ cm^{-3}. (After ref. [50])

6. CONCLUSIONS

In this chapter we have reviewed basic aspects of electron and hole transport in artificially structured 2D systems. The concept of modulation (or selective) doping has provided structures with extremely high electron and hole mobilities. Very significant reductions of impurity scattering in modulation doped systems allowed extensive studies of phonon scattering down to very low temperatures. These studies raise several issues concerning the free carrier screening of acoustic phonon deformation potential. It is now quite evident that the reduced dimensionality is clearly observed only at low temperatures. At higher temperatures of $T > 100$ K charge transport in 2D systems is very similar to that observed in 3D high purity semiconductors. For example, it has been demonstrated that charge confinement does not affect highly inelastic scattering by optical phonons.

Although this review was restricted to lattice matched semiconductor systems, most of the concepts and methods can be easily adopted to lattice mismatched and pseudomorphic systems. At strained semiconductor interfaces an important complication arises from the fact that one has to consider the effect of planar strain on the electronic structure. The effects of the strain are especially complex in the case of the degenerate valence bands. Also, the electronic transport depends on whether the strained layer is unrelaxed, partially, or fully relaxed, since it can be affected by structural defects at the interfaces. All these issues are of great importance for strained GaAs/InGaAs and Si/SiGe heterostructures which are considered the most promising systems for a high performance heterjunction bipolar transistors.

Spectacular improvements in electron and hole mobilities found in AlGaAs/GaAs MDHs are not matched by other semiconductor systems. Interesting and potentialy very promising heterostructures are based on III-V and II-VI narrow band gap compounds Because of very small electron effective mass in these materials one should, in principle, be able to achieve electron mobilities much higher than those in GaAs based heterostructures. The progress in this area will, however, depend on further improvements in the quality of the epitaxial layers of these materials. One of the main problems is still much lower purity of the narrow gap materials compared with GaAs or AlGaAs thin films. In narrow gap II-VI semiconductors, lower than expected mobilities can be also attributed to the difficulty in preparing high quality abrupt heterointerfaces. Reducing of the heterointerface intermixing will be necessary to take full advantage of HgTe or HgSe based modulation doped heterostructures.

Charge transport in 2D systems is now a mature research area with well developed experimental and theoretical methods. Progress in material preparation techniques have made possible to study charge transport in 1D (quantum wires), as well as unusual properties of OD (quantum dot) systems. An intense effort in several laboratories into development of these new methods of preparation of strongly confined low-dimensional systems has already produced a wealth of new results and certainly will be the research area actively pursued in the future.

ACKNOWLEDGEMENTS

The author would like to gratefully acknowledge helpful discussions with E. E. Haller. This work was supported by the Director, Office of Energy Research, Office of Basic Energy Sciences, Materials Science Division of the U.S. Department of Energy under Contract No. DE-AC03-76SF00098.

REFERENCES

[1] K.v. Klitzing, G. Dorda, and M. Pepper, Phys. Rev. Lett. **45**, 494 (1980).
[2] D. Tsui, H. L. Störmer and A.C. Gossard, Phys. Rev. Lett. **48**, 1559 (1982).
[3] S. Schmitt-Rink, D.S. Chemla, and D.A.B. Miller, Adv. Phys. **38**, 89 (1989).
[4] W. Zawadzki, in *Handbook of Semiconductors*, Vol. **1**, edited by W. Paul (North Holland, Amsterdam, 1982) p. 713.
[5] G.E. Stillman and C.M. Wolfe, Thin Solid Films **37**, 69 (1976).
[6] W. Walukiewicz, J. Lagowski, L. Jastrzebski, M. Lichtensteiger, and H.C. Gatos, J. Appl. Phys. **50**, 899 (1979).
[7] R. Dingle, H.L. Störmer, A.C. Gossard, and W. Wiegmann, Appl. Phys. Lett. **33**, 665 (1978).
[8] T.J. Drummond, H. Morkoc, and A.Y. Cho, J. Appl. Phys. **52**, 1380 (1981).
[9] T. Ando, A.B. Fowler, and F. Stern, Rev. Mod. Phys. **54**, 437 (1982).
[10] S. Hiyamizu, in *Semiconductors and Semimetals*, Vol. **30**, edited by R.K. Wiliardson and A.C. Beer, (Academic Press, Inc., Harcourt Brace Jovanovich, Publishers, 1990), p. 53.
[11] H. Morkoc and H. Unlu, in *Semiconductors and Semimetals*, Vol. **24**, edited by R.K. Wiliardson and A.C. Beer, (Academic Press, Inc., Harcourt Brace Jovanovich, Publishers, 1987), p. 135.
[12] D.S. Chemla, D.A.B. Miller, and P.W. Smith, *ibid*, Vol. **24**, p. 279.
[13] W.T. Tseng, *ibid*, Vol. **24**, p.397.
[14] G.C. Osbourn, P.L. Gourley, I.J. Fritz, R.M. Biefeld, L.R. Dawson, and T.E. Zipperian, *ibid*, Vol. **24**, p. 459.
[15] See e.g., F. Stern, and W.E. Howard, Phys. Rev. **163**, 816 (1967).
[16] A. Zrenner, H. Reisinger, F. Koch, K. Ploog, and J.C. Maan, Phys. Rev. B **33**, 5607 (1986).
[17] L. Esaki and K. Tsu, IBM J. Res. Dev. **14**, 61 (1970).
[18] G. Tuttle, H. Kroemer, and J. English, Appl. Phys. Lett. **65**, 5239 (1989).
[19] M. Sundram, A.C. Gossard, J.H. English, and R.M. Westervelt, Superlattices and Microstructures **4**, 683 (1988).
[20] M. Shayegan, T. Sajoto, J. Jo, M. Santos, and C. Silvestre, Appl. Phys. Lett. **53**, 791 (1988).

[21] L. Pfeiffer, K.W. West, H.L. Störmer, and K.W. Baldwin, Appl. Phys. Lett. **55**, 1888 (1989).
[22] T. Saku, Y. Kirayama, and Y. Horikoshi, Jap. J. Appl. Phys. **30**, 902 (1991).
[23] W.I. Wang, E.E. Mendez, Y. Iye, B. Lee, M.H. Kim, and G.E. Stillman, Appl. Phys. Lett. **60**, 1834 (1986).
[24] T. Ando, J. Phys. Soc. Jap. **51**, 3893 (1982).
[25] T. Ando, *ibid*, **51**, 3900 (1982).
[26] W. Walukiewicz, H.E. Ruda, J. Lagowski, and H.C. Gatos, Phys. Rev. B **30**, 4571 (1984).
[27] Y. Okuyama and N. Tokuda, Phys. Rev. B **40**, 9744 (1989).
[28] F. Stern and W.E. Howard, Phys. Rev. **163**, 816 (1967).
[29] U. Ekenberg and M. Altarelli, Phys. Rev. B **30**, 3569 (1984).
[30] D.A. Broido and L.J. Sham, Phys. Rev. B **31**, 888 (1985).
[31] T. Ando, J. Phys. Soc. Japan **54**, 1528 (1985).
[32] W. Walukiewicz, Phys. Rev. B **31**, 5557 (1985).
[33] See e.g., D.J. Howarth and E.H. Sondheimer, Proc. Phys. Soc. London A **219**, 53 (1953).
[34] D.L. Rode, in *Semiconductors and Semimetals*, Vol. **10**, edited by R.K Wiliardson and A.C. Beer, (Academic Press, Inc., Harcourt Brace Jovanovich, Publishers, 1975), Chap. 1.
[35] P.J. Price, Annals of Physics **133**, 217 (1981).
[36] B.K. Ridley, J. Phys. C: Solid State Phys. **15**, 5899 (1982).
[37] V. Karpus, Sov. Phys. Semicon. **20**, 6 (1986).
[38] W. Walukiewicz, Phys. Rev. B **37**, 8530 (1988).
[39] Y. Okuyama and N. Tokuda, Phys. Rev. B **42**, 7028 (1990).
[40] P.J. Price, Surf. Sci. **143**, 145 (1984).
[41] T. Kawamura and S. Das Sarma, Phys. Rev. B **45**, 3612 (1992).
[42] P.J. Price, Solid State Comm. **51**, 607 (1984).
[43] H.L. Stromer, L.N. Prfieer, K.W. Baldwin, and K. West, Phys. Rev. B **41**, 1278 (1990).
[44] V. Karpus, Semicon. Sci. Technol. **5**, 691 (1990).
[45] B. Vinter, Appl. Phys. Lett. **45**, 581 (1984).
[46] H.J. Polland, W.W. Rühle, K. Ploog, and C.W. Tu, Phys. Rev. B **36**, 7722 (1987).
[47] L. Makowski and M. Glicksman, J. Phys. Chem. Solids **34**, 487 (1973).
[48] G. Bastard, Appl. Phys. Lett. **43**, 591 (1983).
[49] A. Hartstein, T.H. Ning, and A.B. Fowler, Surf. Sci. 58, 178 (1976).
[50] W. Walukiewicz, P.F. Hopkins, M. Sundaram,. and A.C. Gossard, Phys. Rev. B 44, 10 909 (1991).
[51] H. Sakaki, T. Noda, K. Hirakawa, M. Tanaka, and T. Matsusne, Appl. Phys. Lett. **51**, 1934 (1987).
[52] H. Morkoc, T.J. Drummond, and R. Fischer, Appl. Phys. **53**, 1030 (1982).
[53] S. Mori and T. Ando, Phys. Rev. B **19**, 6433 (1979).

[54] N.T. Thang, G. Fishman, and B. Vinter, Surf. Sci. **142**, 266 (1984).
[55] H.L. Stormer, K. Baldwin, A.C. Gossard, and W. Wiegmann, Appl. Phys. Lett. **44**, 1062 (1984).
[56] W.I. Wang, E.E. Mendez, and F. Stern, Appl. Phys. Lett. **45**, 639 (1984).
[57] E.E. Mendez and W.I. Wang, Appl. Phys. Lett. **46**, 639 (1985).
[58] W. Walukiewicz, J. Appl. Phys. **53**, 3577 (1986).
[59] G.E. Pikus and G.L. Bir, Sov. Phys., Solid State Phys. **1**, 1502 (1958).
[60] E. Gwinn, P.F. Hopkins, A.J. Rimberg, K.M. Westervelt, M. Sundaram, and A.C. Gossard, Phys. Rev. B **41**, 10700 (1990).
[61] K. Fuchs, Proc. Cambridge Philos. Soc. **34**, 100 (1938).
[62] J.R. Schrieffer, Phys. Rev. **97**, 641 (1955).
[63] A.A. Cottey, Thin Solid Films **1**, 297 (1967).
[64] S.B. Soffer, J. Appl. Phys. **38**, 1710 (1967).
[65] H. Morkoc, T.J. Drummond, and R. Fischer, J. Appl. Phys. **53**, 1030 (1982).
[66] S. Sasa, J. Saito, K. Nanbu, T. Ishikawa, and S. Hiyamizu, Jpn. J. Appl. Phys. **23**, L573 (1984).
[67] W. Walukiewicz and E.E. Haller, Appl. Phys. Lett. **58**, 1638 (1991).
[68] W. Walukiewicz, Appl. Phys. Lett. **54**, 2094 (1989).
[69] U. Meirav, M. Heiblum, and F. Stern, Appl. Phys. Lett. **52**, 1268 (1988).
[70] For recent review see e.g. D.V. Lang in *Deep Levels in Semiconductors*, edited by S.T. Pandelides (Gordon and Breach Science Publishers, New York, 1986) p. 489.
[71] H.L. Stormer, A.C. Gossard, and W. Wiegmann, Solid State Comm. **41**, 707 (1982).
[72] D.R. Leadley, R.J. Nicholas, J.J. Harris, and C.T. Foxon, Semicon. Sci. Techn. **5**, 1081 (1990).
[73] R. Fletcher, E. Zaremba, M. DiIorio, C.T. Foxon, and J.J. Harris, Phys. Rev. B **38**, 7866 (1988).
[74] A. Kastalsky, R. Dingle, K.Y. Cheng, and A.Y. Cho, Appl. Phys. Lett. **41**, 279 (1982).
[75] M.A. Tischler and B.D. Parker, Appl. Phys. Lett. **58**, 1614 (1991).
[76] M. Takikawa, J. Komeno, and M. Ozeki, Appl. Phys. Lett. **43**, 280 (1983).
[77] Y. Takeda and A. Sakaki, Jap. J. Appl. Phys. **24**, 1307 (1985).
[78] J.R. Hayes, A.R. Adams, and P.D. Greene in *GaInAsP Alloy Semiconductors*, edited by T.P. Pearsall (Wiley, New York, 1982).
[79] E.E. Mendez, P.J. Price, and M. Heiblum, Appl. Phys. Lett. **45**, 294 (1984).
[80] P.J. Price, Phys. Rev. B **32**, 2643 (1985).
[81] W. Walukiewicz, H.E. Ruda, J. Lagowski, and H.C. Gatos, Phys. Rev. B **32**, 2465 (1985).
[82] D.D. Nolte, W. Walukiewicz, and E.E. Haller, Phys. Rev. Lett. **59**, 501 (1984).

[83] C.G. Van de Walle and R.M. Martin, Phys. Rev. Lett. **62**, 2028 (1989).
[84] J. H. English, A.C. Gossard, H. L. Störmer and K. W. Baldwin, Appl. Phys. Lett., **50**, 1826, (1987).

LAWRENCE BERKELEY LABORATORY
CENTER FOR ADVANCED MATERIALS
1 CYCLOTRON ROAD
BERKELEY, CALIFORNIA 94720